NASA/TM–2019–220262

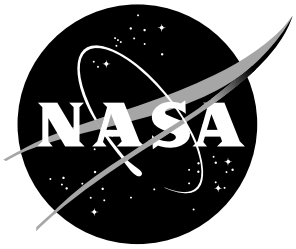

Flow Resistance Comparative Study

Martha C. Brown, Michael G. Jones, and Brian M. Howerton
Langley Research Center, Hampton, Virginia 23681

Asif Syed and Luke Shafer
University of Cincinnati, Cincinnati, Ohio 45221

Fumitaka Ichihashi and Lisa Bowen
Hexcel Corporation, Casa Grande, Arizona 85122

March 2019

NASA STI Program. . . in Profile

Since its founding, NASA has been dedicated to the advancement of aeronautics and space science. The NASA scientific and technical information (STI) program plays a key part in helping NASA maintain this important role.

The NASA STI Program operates under the auspices of the Agency Chief Information Officer. It collects, organizes, provides for archiving, and disseminates NASA's STI. The NASA STI Program provides access to the NASA Aeronautics and Space Database and its public interface, the NASA Technical Report Server, thus providing one of the largest collection of aeronautical and space science STI in the world. Results are published in both non-NASA channels and by NASA in the NASA STI Report Series, which includes the following report types:

- TECHNICAL PUBLICATION. Reports of completed research or a major significant phase of research that present the results of NASA programs and include extensive data or theoretical analysis. Includes compilations of significant scientific and technical data and information deemed to be of continuing reference value. NASA counterpart of peer-reviewed formal professional papers, but having less stringent limitations on manuscript length and extent of graphic presentations.
- TECHNICAL MEMORANDUM. Scientific and technical findings that are preliminary or of specialized interest, e.g., quick release reports, working papers, and bibliographies that contain minimal annotation. Does not contain extensive analysis.
- CONTRACTOR REPORT. Scientific and technical findings by NASA-sponsored contractors and grantees.
- CONFERENCE PUBLICATION. Collected papers from scientific and technical conferences, symposia, seminars, or other meetings sponsored or co-sponsored by NASA.
- SPECIAL PUBLICATION. Scientific, technical, or historical information from NASA programs, projects, and missions, often concerned with subjects having substantial public interest.
- TECHNICAL TRANSLATION. English-language translations of foreign scientific and technical material pertinent to NASA's mission.

Specialized services also include organizing and publishing research results, distributing specialized research announcements and feeds, providing information desk and personal search support, and enabling data exchange services.

For more information about the NASA STI Program, see the following:

- Access the NASA STI program home page at `http://www.sti.nasa.gov`
- E-mail your question to `help@sti.nasa.gov`
- Phone the NASA STI Information Desk at 757-864-9658
- Write to:
  NASA STI Information Desk
  Mail Stop 148
  NASA Langley Research Center
  Hampton, VA 23681-2199

NASA/TM–2019–220262

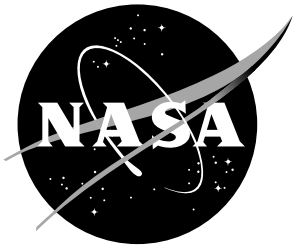

Flow Resistance Comparative Study

Martha C. Brown, Michael G. Jones, and Brian M. Howerton
Langley Research Center, Hampton, Virginia 23681

Asif Syed and Luke Shafer
University of Cincinnati, Cincinnati, Ohio 45221

Fumitaka Ichihashi and Lisa Bowen
Hexcel Corporation, Casa Grande, Arizona 85122

National Aeronautics and
Space Administration

Langley Research Center, Hampton, Virginia 23681

March 2019

Acknowledgments

This work was funded by the Advanced Air Transport Technology Project of the NASA Advanced Air Vehicles Program.

Available from:

NASA STI Program / Mail Stop 148
NASA Langley Research Center
Hampton, VA 23681-2199
Fax: 757-864-6500

Abstract

This study presents the DC flow resistance results of nine (9) samples acquired using raylometers at three research facilities: NASA Langley Research Center, University of Cincinnati, and the Hexcel Corporation. DC flow resistance is the acoustic resistance component of acoustic impedance of a liner at zero frequency. This DC flow resistance represents a good approximation for acoustic resistance at frequencies away from resonance and anti-resonance, and is therefore useful to the liner designer as an initial estimate of the acoustic resistance. The samples included in this study are comprised of six perforates (three micro-perforates and three conventional perforates) and three wire meshes (varying in flow resistance). Although each of the raylometers used by the three facilities are different in physical characteristics and employ different testing methodologies, the results compare favorably.

1 Introduction

For nearly five decades, passive acoustic liners have been a key contributor in the reduction of fan noise propagated through the inlet and aft-fan duct of aircraft engine nacelles. These liners often consist of single layer perforate-over-honeycomb structures (Figure 1). The most pertinent parameter for understanding the acoustic performance of these liners is the acoustic impedance, an intrinsic parameter that is defined as the ratio of the acoustic pressure to the normal component of acoustic particle velocity at the liner surface. The acoustic impedance consists of a real component, acoustic resistance, and an imaginary component, acoustic reactance. The acoustic reactance is largely a function of the thickness (height) of the honeycomb core, and its value determines whether impinging sound waves can penetrate into the acoustic liner. The acoustic resistance is dominated by the facesheet and septum properties. Many models exist to predict these properties, but one of the simpler experimental methods for comparison of perforates and wire meshes is to use a raylometer to measure their DC flow resistances. DC flow resistance is the acoustic resistance component of acoustic impedance of a liner at zero frequency. This DC flow resistance is generally a good approximation of the acoustic resistance presented by the liner at frequencies away from resonance and anti-resonance, and is therefore useful as an initial estimate of the acoustic resistance for the liner designer.

This study presents the DC flow resistance results of nine (9) samples acquired using raylometers at three research facilities: NASA Langley Research Center, University of Cincinnati, and the Hexcel Corporation. The purpose of the current investigation is to compare the DC flow resistance results achieved in three facilities that employ diverse raylometers and testing methodologies. These three unique facilities are used to evaluate a set of perforate and wire mesh samples, such that direct comparisons can be used to evaluate the effects of the different measurement processes on the estimates of the DC flow resistance. The nine samples included in this study are comprised of six perforates (three micro-perforates and three conventional per-

forates) and three wire meshes (varying in flow resistance). Although each of the raylometers used by the three facilities are different in physical characteristics and employ different testing methodologies, the results compare favorably.

2 Acoustic Impedance Modeling

For single-layer perforate-over-honeycomb liners, the impedance can be modeled as follows [1]:

$$\zeta = \theta + i\chi = \theta_{linear} + \theta_{nonlinear} + \theta_{gf} + i\left\{\chi_{fs} - cot\left(kh\right)\right\} \tag{1}$$

where θ_{linear} and $\theta_{nonlinear}$ are the linear (viscous) and nonlinear contributions to the facesheet resistance, respectively, and θ_{gf} is the grazing flow contribution to the acoustic resistance. The reactance is given by the expression in brackets, and it includes the effects of the facesheet (mass reactance, χ_{fs}) and the cavity height $[-cot(kh)]$ (where k is the free space wave number and (ω/c) and h is the height of the liner). Note that an $e^{i\omega t}$ time convention is used (where ω is the angular frequency and t is time), and all impedances are normalized by ρc (where ρ is the ambient density and c is the ambient speed of sound). This study focuses on the facesheet resistance, i.e., the combination of θ_{linear} and $\theta_{nonlinear}$.

3 DC Flow Resistance

"A lumped-element assumption for a perforate plate allows the acoustic oscillatory flow through the perforate to be treated as locally incompressible and quasi-steady. Thus, a DC flow resistance measurement on the perforate provides the basis for an empirical model of the acoustic resistance. [1]" The normalized DC flow resistance, θ_f, is given by:

$$\theta_f = R_f/\rho c = A + B * V \tag{2}$$

where R_f is the dimensional DC flow resistance, constant A is the DC flow component, constant B is the nonlinear contribution to the flow resistance (i.e., A and B are directly related to θ_{linear} and $\theta_{nonlinear}$, respectively), and $V_{incident}$ is the measured incident flow velocity through the facesheet sample. For a purely linear liner, $B = 0$. However, in practice, most acoustic liner components are weakly nonlinear, i.e., the B term is larger than zero. Experimentally, R_f is determined using:

$$R_f = \Delta P_s/V_{incident} \tag{3}$$

where ΔP_s is the measured pressure drop across the facesheet sample. This measurement is conducted in the raylometer. Such measurements should be conducted over an incident velocity range commensurate with that expected for the source sound pressure level expected to be present in the final (e.g., aircraft engine nacelle) application. The constants A and B can be determined directly by fitting Equation (2) to the measured values of R_f and $V_{incident}$.

This process is repeated multiple times for each sample in the current investigation, in order to use statistical methods to evaluate the uncertainty associated with the measurement processes. Also, both sides of each sample are tested to determine manufacturing effects on the flow resistance. In the current paper, these tests are labeled as "Push," where the flow impinges on Side A, and "Pull," where the flow impinges on Side B (see Figure 2). Side B is achieved by physically flipping the sample.

For the current investigation, the DC flow resistance, R_f, of a perforate or wire mesh sample is measured over a range of incident velocities, $V_{incident}$, from approximately 20 to 200 cm/s. It is fairly common practice in industry to specify the flow resistance of a material by the flow resistance measured at 105 cm/s, R_{105} (i.e., at the midpoint in the velocity range of measurement).

4 Nonlinearity Factor

A liner is classified as linear when the acoustic performance is independent of the normal component of the acoustic particle velocity. Because of the interdependence of the acoustic particle velocity and the acoustic pressure amplitude, a linear liner is also independent of the amplitude of the sound field. The nonlinearity factor (NLF) of a liner is almost entirely determined by the acoustic properties of the facesheet, and is computed as:

$$NLF = \frac{R_{200}}{R_{20}} \tag{4}$$

where R_{200} and R_{20} are the DC flow resistances in cgs Rayl at 200 cm/s and 20 cm/s, respectively. It is fairly common practice in industry to characterize a sample as linear, weakly nonlinear, or nonliner based on NLF. As mentioned earlier, a linear liner would have an NLF equal to 1, but most conventional liners have higher NLF values, and are thus classified as weakly nonlinear.

The NLF parameter provides insight into equation (2). If the NLF is unity, B has a value of zero. If the NLF is large, the B term becomes dominant and the A term becomes negligible.

Three types of samples are used in this study. These include conventional perforates, microperforates, and wire meshes. These were chosen to cover a range of sheet thickness, t, to hole diameter, d, ratios. The conventional perforates used in this study have t/d ratios near unity. The microperforates have t/d ratios of 5, and the wire meshes have t/d ratios near 6. The corresponding nonlinearity factors, NLF, are expected to decrease as the t/d ratio increases. The objective of this study is to compare the results of conventional, microperforate, and wire mesh facesheets among the three facilities.

Another parameter that affects the nonlinearity factor is the shape of the perforation. Depending on the method used for fabrication, the shape of the perforation may deviate from the clean, conical shape. As the "edge" of the perforation upon which the flow impinges becomes sufficiently sharp, the nonlinearity will increase.

As mentioned earlier, samples were tested using the "Push" and "Pull" approaches. This allows these effects of the manufacturing process to be assessed. The results measured for the two sides are expected to be very similar for samples with nonlinearity factors near unity, and to diverge as the NLF grows well above unity.

5 Uncertainty Metrics

For this study, the metric for uncertainty is chosen to be the 95% confidence interval [2]. This interval is calculated from the statistics generated by repeated DC flow resistance measurements. Calculation of 95% confidence intervals within this study assumes input parameter statistics to be Gaussian distributed. These confidence intervals are deemed to have a 95-percent probability of containing the "truth."

When estimating a confidence interval for a small trial size ($N < 32$) taken from a normally distributed parent population, a coverage factor is introduced to account for the fact that the sample probability density function follows a Student's t-distribution for small sample sizes [2].

6 Description of Test Rigs

Figure 3 provides photographs of each of the raylometers used in this investigation. It should be noted that each of these test rigs is capable of being reconfigured for different applications. For the purposes of this study, the NASA and University of Cincinnati raylometers were configured to use 2.0"x2.0" square samples, whereas the Hexcel raylometer was configured to use 3.14"-diameter circular samples. All samples used among the three facilities were prepared from the same parent materials.

7 Description of Samples

Figures 4a, 4b, and 4c are photographs of representative microperforate, conventional, and wire mesh facesheet samples, respectively. Table 1 outlines the characteristics of each of the nine (9) samples. The nomenclature is defined by sample name, the type of sample, porosity in percent open area (POA), facesheet hole diameter (d), facesheet thickness (t), thickness to diameter ration (t/d), and facesheet description.

Table 1: Test Sample Description.

Sample	Type	POA(%)	d (in)	t (in)	t/d	Description
MP1	Perforate	5%	0.010	0.050	5.00	Microperforate
MP2	Perforate	10%	0.010	0.050	5.00	Microperforate
MP3	Perforate	15%	0.010	0.050	5.00	Microperforate
UC1	Perforate	6.2%	0.039	0.025	0.64	Conventional
UC2	Perforate	10.03%	0.040	0.041	1.00	Conventional
UC3	Perforate	9.82%	0.040	0.075	1.90	Conventional
WM1	Mesh	-	-	-	-	(SEFAR 15) 15 cgs rayls, nominal
WM2	Mesh	-	-	-	-	(SEFAR 27) 27 cgs rayls, nominal
WM3	Mesh	-	-	-	-	(SEFAR 42) 42 cgs rayls, nominal

8 Test Matrix

Each facility utilized slightly different test matrices. NASA performed 11 trials for each test sample with 10 evenly spaced data points ranging from 20 cm/s to 200 cm/s in 20 cm/s increments. The University of Cincinnati performed 10 trials for each test sample with 10 data points at nominally the same velocities as NASA. Hexcel performed 11 trials of each test sample and added one additional velocity at 220 cm/s.

9 Results

The flow resistance results for each sample acquired among the three laboratories are listed in the Appendices. The calculated flow resistance of the sample (R_{105}) and nonlinearity factor (NLF) are listed with 95% confidence intervals as computed from raw measured data. Uncertainties are based on the standard deviation of resistance. Results acquired with the air impinging on each sample side (PUSH-A and PULL-B, respectively) are provided.

R_{105} values, along with their corresponding uncertainty intervals, are provided in cgs rayls. The corresponding NLF values and related uncertainty intervals are non-dimensional. Also, it should be noted that the data in this report have been corrected to standard day conditions (i.e., 70^oF, 14.7 psia). R_{105} and NLF are commonly used in the liner community when characterizing a facesheet sample.

Microperforate facesheets have the thickness of the facesheet much larger than the hole diameters ($t/d > 1$). Samples MP1, MP3, and MP3 are classified as microperforate facesheets since $t/d = 5.00$. Results are presented in Tables A1, A2, and A3 respectively. These facesheets are more linear than conventional facesheets, as the nonlinear factor (NLF) approaches unity as the porosity increases, for a fixed hole diameter, d. Results from both sides of the facesheet yield similar results.

The reader should note that each sample was removed and installed for each trial and there were differences in sample size among the three facilities. Therefore, it

is presumed that much of the differences in the flow resistance results are due to installation effects.

Results among the three laboratories yield favorable comparisons, within their respective uncertainty bands. For example, the R_{105} value decreases with increasing POA, meaning as the porosity increases, flow resistance decreases and the NLF approach unity. The three facilities provide very similar results.

Conventional perforate facesheets, with $t/d \sim 1$, are typically classified as weakly nonlinear ($NLF > 1$). Samples UC1, UC2, and UC3 are conventional perforate facesheets. Results are presented in Tables B1, B2, and B3 respectively. Results for these facesheets from Side A and Side B are similar. Differences among each laboratory are comparable. Each result exhibits small confidence intervals.

Wire meshes are predicted to be nearly linear ($NLF \sim 1$). Samples WM1, WM2, and WM3 are wire meshes. Results are presented in Tables C1, C2, and C3 respectively. Note that all samples follow the expected characteristics of a wire mesh as all results for Side A and Side B are nearly identical (very near unity). Small confidence intervals demonstrate the good precision of the measurement of each laboratory. All values are similar, indicating all three laboratories present comparative results.

10 Concluding Remarks

This study presents the flow resistance results of nine (9) samples acquired using raylometers at three research facilities: NASA Langley Research Center, University of Cincinnati, and the Hexcel Corporation. Although each of the raylometers used by the three facilities are different in physical characteristics and employ different testing methodologies, the results are comparable among the facilities and the trends are similar. There are some measurable differences when comparing University of Cincinnati to NASA and Hexel Corporation to NASA. However, considering the same parent material was used, any differences although small, are believed due to installation effects.

References

1. Parrott, T. L. and Jones, M. G., "Assessment of NASA's Aircraft Noise Prediction Capability, Chapter 6: Uncertainty in Acoustic Liner Impedance Measurement and Prediction," NASA TP 2012-215653, July 2012.

2. Coleman, H. W. and Steele, W. G., *Experimentation and Uncertainty Analysis for Engineers*, John Wiley & Sons, 1989.

Figures

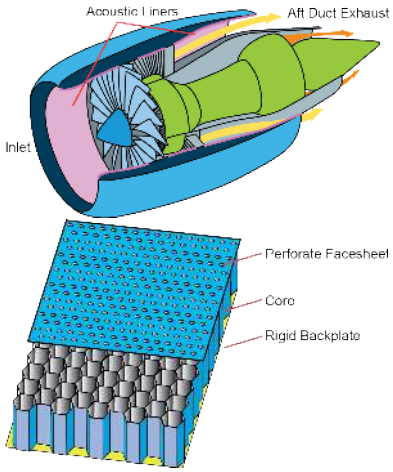

Figure 1: Sketches of liners as installed in engine (top figure) and conventional liner characteristics (bottom figure).

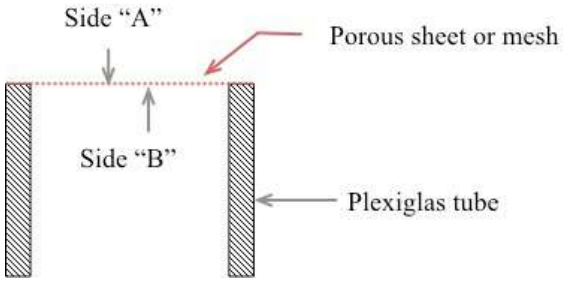

Figure 2: Illustration of perforate plate installation in a Raylometer (DC flow resistance test rig).

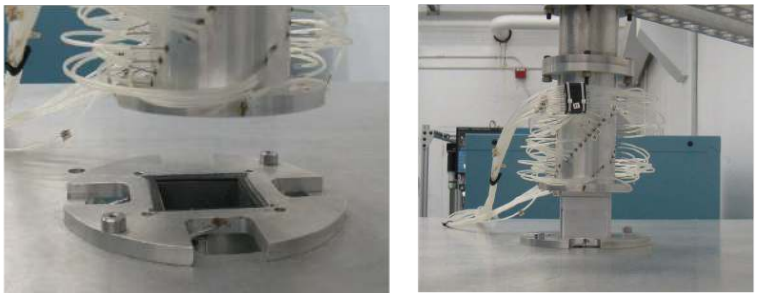

NASA LaRC Raylometer

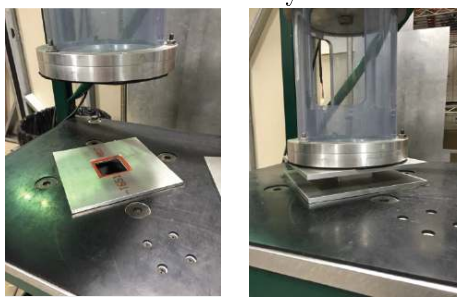

University of Cincinnati Raylometer

Hexcel Raylometer

Figure 3: Photographs of the NASA LaRC, University of Cincinnati, and Hexcel raylometers, respectively.

(a) Sample MP1.

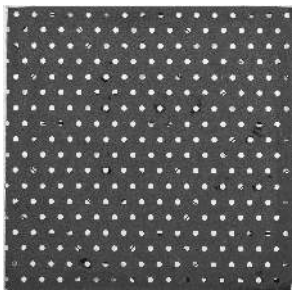

(b) Sample UC1.

(c) Sample WM1.

Figure 4: Facesheet sample representations.

The following appendices contain the results of the calculated flow resistance of each respective facesheet sample, R_{105} in cgs Rayl and nonlinearlity factor, NLF (dimensionless). Note that these parameters are used in general liner design when characterizing a facesheet material. Results for each facility are noted on the same page so the reader can compare results, qualitatively. Note the objective of this study is to compare the trends of conventional, microperforate, and wire mesh facesheets among these three facilities.

Appendix A

Microperforate Results

Table A1: Sample MP1.

Microperforate, POA=5, d=0.01 in., t=0.050 in., $t/d = 5.00$

PUSH-A	NASA	UC	Hexcel
R_{105}	45.95 ±0.07	48.08 ±0.06	42.67 ±0.05
NLF	3.29 ±0.01	3.34 ±0.02	3.27 ±0.01

PULL-B	NASA	UC	Hexcel
R_{105}	42.31 ±0.01	48.03 ±0.05	45.24 ±0.06
NLF	2.99 ±0.00	3.13 ±0.01	3.03 ±0.01

Table A2: Sample MP2.

Microperforate, POA=10, d=0.01 in., t=0.050 in., $t/d = 5.00$

PUSH-A	NASA	UC	Hexcel
R_{105}	14.93 ±0.01	15.02 ±0.05	15.50 ±0.02
NLF	2.40 ±0.01	2.43 ±0.01	2.44 ±0.01

PULL-B	NASA	UC	Hexcel
R_{105}	14.68 ±0.01	15.25 ±0.03	15.05 ±0.01
NLF	2.35 ±0.01	2.36 ±0.01	2.39 ±0.01

Table A3: Sample MP3.

Microperforate, POA=15, d=0.01 in.,t=0.050 in., $t/d = 5.00$

PUSH-A	NASA	UC	Hexcel
R_{105}	9.07 ±0.01	9.33 ±0.02	9.31±0.04
NLF	1.91 ±0.01	1.94 ±0.005	1.99±0.01

PULL-B	NASA	UC	Hexcel
R_{105}	9.64 ±0.01	9.91 ±0.01	9.88 ±0.01
NLF	2.05 ±0.01	2.10 ±0.005	2.18 ±0.01

Appendix B

Conventional Perforate Results

Table B1: Sample UC1.

Perforate, POA=6.2, d=0.039 in., t=0.025 in., $t/d = 0.64$

PUSH-A	NASA	UC	Hexcel
R_{105}	22.06 ±0.01	22.12 ±0.04	23.29 ±0.03
NLF	10.35 ±0.08	10.53 ±0.11	11.09 ±0.11

PULL-B	NASA	UC	Hexcel
R_{105}	23.55 ±0.05	23.91 ±0.02	25.45 ±0.03
NLF	13.64 ±0.32	14.90 ±0.07	15.10±0.19

Table B2: Sample UC2.

Perforate, POA=10.03, d=0.040 in., t=0.041 in., $t/d = 1.00$

PUSH-A	NASA	UC	Hexcel
R_{105}	9.28 ±0.01	9.51 ±0.01	9.74 ±0.01
NLF	6.34 ±0.03	6.07 ±0.06	7.70 ±0.14

PULL-B	NASA	UC	Hexcel
R_{105}	9.42 ±0.02	9.59 ±0.01	9.85 ±0.02
NLF	5.48 ±0.06	6.42 ±0.03	8.20 ±0.13

Table B3: Sample UC3.

Perforate, POA=9.82, d=0.40 in., t=0.075 in., $t/d = 1.90$

PUSH-A	NASA	UC	Hexcel
R_{105}	10.43 ±0.01	9.99 ±0.01	10.16±0.01
NLF	5.92 ±0.03	6.02 ±0.02	7.62±0.13

PULL-B	NASA	UC	Hexcel
R_{105}	9.84 ±0.02	9.95 ±0.00	10.14 ±0.01
NLF	6.37 ±0.09	6.63 ±0.03	8.52 ±0.08

Appendix C

Wire Mesh Results

Table C1: Sample WM1.
Wire Mesh, SEFAR15, 15 cgs rayls

PUSH-A	NASA	UC	Hexcel
R_{105}	15.08 ±0.02	15.53 ±0.03	15.57 ±0.03
NLF	1.14 ±0.01	1.15 ±0.00	1.15 ±0.00

PULL-B	NASA	UC	Hexcel
R_{105}	15.47 ±0.01	15.50 ±0.02	15.68 ±0.02
NLF	1.13 ±0.00	1.15 ±0.00	1.15±0.00

Table C2: Sample WM2.
Wire Mesh, SEFAR 27, 27 cgs rayls

PUSH-A	NASA	UC	Hexcel
R_{105}	27.73 ±0.02	28.06 ±0.02	28.31 ±0.03
NLF	1.11 ±0.00	1.12 ±0.00	1.10 ±0.00

PULL-B	NASA	UC	Hexcel
R_{105}	27.51 ±0.02	28.08 ±0.08	28.19 ±0.03
NLF	1.11 ±0.00	1.13 ±0.00	1.10 ±0.00

Table C3: Sample WM3.
Wire Mesh, SEFAR 42, 42 cgs rayls

PUSH-A	NASA	UC	Hexcel
R_{105}	44.69 ±0.02	45.40 ±0.10	46.06±0.02
NLF	1.10 ±0.00	1.12 ±0.00	1.08±0.00

PULL-B	NASA	UC	Hexcel
R_{105}	45.32 ±0.03	45.36 ±0.09	46.04 ±0.05
NLF	1.09 ±0.00	1.11 ±0.00	1.07 ±0.00

REPORT DOCUMENTATION PAGE

Form Approved
OMB No. 0704–0188

1. REPORT DATE *(DD-MM-YYYY)*	2. REPORT TYPE	3. DATES COVERED *(From - To)*
01-03-2019	Technical Memorandum	

4. TITLE AND SUBTITLE
Flow Resistance Comparative Study

5a. CONTRACT NUMBER

5b. GRANT NUMBER

5c. PROGRAM ELEMENT NUMBER

6. AUTHOR(S)
Brown, Martha C.; Jones, Michael G.; Howerton, Brian M.; Syed, Asif; Shafer, Luke; Ichihashi, Fumitaka; Bowen, Lisa

5d. PROJECT NUMBER

5e. TASK NUMBER

5f. WORK UNIT NUMBER
081876.02.07.03.01.01

7. PERFORMING ORGANIZATION NAME(S) AND ADDRESS(ES)
NASA Langley Research Center, Hampton, Virginia 23681

8. PERFORMING ORGANIZATION REPORT NUMBER
L–21009

9. SPONSORING/MONITORING AGENCY NAME(S) AND ADDRESS(ES)
National Aeronautics and Space Administration
Washington, DC 20546-0001

10. SPONSOR/MONITOR'S ACRONYM(S)
NASA

11. SPONSOR/MONITOR'S REPORT NUMBER(S)
NASA/TM–2019–220262

12. DISTRIBUTION/AVAILABILITY STATEMENT
Unclassified-Unlimited
Subject Category 71
Availability: NASA STI Program (757) 864-9658

13. SUPPLEMENTARY NOTES
.

14. ABSTRACT
This study presents the DC flow resistance results of nine (9) samples acquired using raylometers at three research facilities: NASA Langley Research Center, University of Cincinnati, and the Hexcel Corporation. DC flow resistance is the acoustic resistance component of acoustic impedance of a liner at zero frequency. This DC flow resistance represents a good approximation for acoustic resistance at frequencies away from resonance and anti-resonance, and is therefore useful to the liner designer as an initial estimate of the acoustic resistance. The samples included in this study are comprised of six perforates (three micro-perforates and three conventional perforates) and three wire meshes (varying in flow resistance). Although each of the raylometers used by the three facilities are different in physical characteristics and employ different testing methodologies, the results compare favorably.

15. SUBJECT TERMS
liner, raylometer, flow resistance, perforate, microperforate

16. SECURITY CLASSIFICATION OF:			17. LIMITATION OF ABSTRACT	18. NUMBER OF PAGES	19a. NAME OF RESPONSIBLE PERSON
a. REPORT	b. ABSTRACT	c. THIS PAGE			STI Information Desk (help@sti.nasa.gov)
U	U	U	UU	18	19b. TELEPHONE NUMBER *(Include area code)* (757) 864-9658